ACS APPLIED MATERIALS & INTERFACES

Research Article

www.acsami.org

Amine-Tethered Adsorbents Based on Three-Dimensional Macroporous Silica for CO_2 Capture from Simulated Flue Gas and Air

Fa-Qian Liu,*[,†] Lei Wang,[‡] Zhao-Ge Huang,[†] Chao-Qin Li,[†] Wei Li,[†] Rong-Xun Li,[†] and Wei-Hua Li[§]

[†]Engineering Research Center of High Performance Polymer and Molding Technology, Ministry of Education, and [‡]College of Chemistry and Molecular Engineering, Qingdao University of Science and Technology, Qingdao 266042, China

[§]Institute of Oceanology, Chinese Academy of Sciences, Qingdao 266071, China

Supporting Information

ABSTRACT: New covalently tethered CO_2 adsorbents are synthesized through the in situ polymerization of N-carboxyanhydride (NCA) of L-alanine from amine-functionalized three-dimensional (3D) interconnected macroporous silica (MPS). The interconnected macropores provide low-resistant pathways for the diffusion of CO_2 molecules, while the abundant mesopores ensure the high pore volume. The adsorbents exhibit high molecular weight (of up to 13058 Da), high amine loading (more than 10.98 mmol N g^{-1}), fast CO_2 capture kinetics ($t_{1/2}$ < 1 min), high adsorption capacity (of up to 3.86 mmol CO_2 g^{-1} in simulated flue gas and 2.65 mmol CO_2 g^{-1} in simulated ambient air under 1 atm of dry CO_2), as well as good stability over 120 adsorption−desorption cycles, which allows the overall CO_2 capture process to be promising and sustainable.

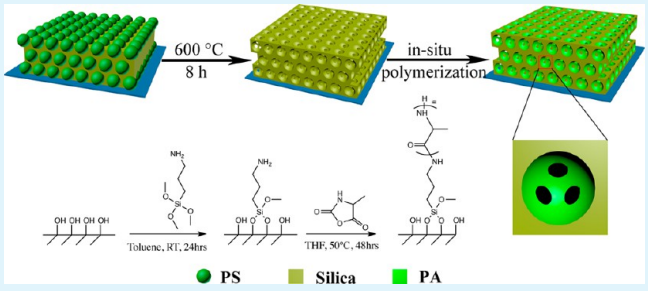

KEYWORDS: *CO_2 capture, amine-tethered adsorbents, macroporous silica, flue gas*

INTRODUCTION

Driven by the increasing concentration of greenhouse gases responsible for global warming, technologies for CO_2 capture and sequestration (CCS) have been extensively developed during the past decade.[1−3] Liquid-amine-based solution CO_2 absorption/desorption systems are presently one of the most suitable technologies for large-scale separation of CO_2 from flue gas streams.[4] However, although these systems are effective, they suffer from numerous drawbacks such as high energy consumption, corrosion, and limited amine concentration in the aqueous phase because of viscosity and foaming issues.[5,6] Recently, solid adsorbents functionalized or impregnated with amines were designed to ameliorate this problem by removing amines from aqueous solution and affixing them to solid supports (porous silicas, carbons, organic resins, and polymers).[7] In contrast to amine scrubbers, solid-supported amine adsorbents offer significant advantages for CO_2 capture, including lower energy cost for adsorbent regeneration and potential elimination of corrosion problems. They also exhibit high selectivity for CO_2 capture because of the specific CO_2−amine chemistry.[8] Among them, mesoporous silica-supported amines with high pore volumes and large surface areas have been extensively studied in the past decade,[2,3,9−11] partly because that silica supports have been found to be relatively stable using the conditions under which they have been tested so far,[12] with the exception of a recent report by Jones.[13]

The array of silica-supported amine adsorbents has been previously categorized into three groups: physical impregnation, covalently tethering, and in situ polymerization within the pores.[12,14] However, these materials generally suffer from low CO_2 capacities or lack stability over many cycles, especially when amines are physisorbed onto the support.[12] The large adsorption capacity (higher than the threshold to economically compete with the amine-scrubbing process), fast kinetics and high stability in the regeneration process, which often demand fundamentally opposing requirements for the design of the adsorbents, still remain the principle hurdle for the mesoporous silica-supported amine adsorbent.[9,15]

To overcome this challenge, it is necessary to design a new paradigm to mitigate the contradiction. Macroporous silica (>50 nm with 1, 2, or 3 dimensionality), which has interconnected pores and high pore volume, represents a special class of materials which are of interest in the fields of medicine, pharmaceutics and materials science; they find diverse applications, including the separation, catalysis and drug delivery.[16,17] In this paper, contrary to the mesoporous adsorbents (2−50 nm), we demonstrate it is advantageous to use the macroporous silica (MPS)-supported amine as the new adsorbent. First, the macroporous adsorbents (>50 nm) are less susceptible to pore blockage and plugging as the amine loading increases,[18−21] while still remain a large pore volume to ensure the rapid kinetics.[22] Second, the molecular weight of the polyamines grafted to the mesoporous silica is low because of the confinement effects of the mesopores.[23] MPS support can

Received: January 6, 2014
Accepted: March 3, 2014
Published: March 3, 2014

   dx.doi.org/10.1021/am500089g | ACS Appl. Mater. Interfaces 2014, 6, 4371−4381

provide enough space for the growth of the polyamine chains, hence improving the amine loading and adsorption capacity. Furthermore, the 3D interconnected macroporous structure with large cell diameter and large aperture diameter networks provides highly interconnected channels that ensure enhanced mass transfer of CO_2 to the adsorption sites.[8]

In continuation with our objective to develop sustainable protocols using morphologically controlled functionalized nanomaterials,[24,25] herein, we report the use of MPS-supported amine as novel adsorbent for CO_2 capture. The macroporous silica was prepared using a simple one-step sol−gel process. Linear poly-L-alanine (PA) was prepared from the in situ polymerization of L-alanine to provide strong covalent links between the amines and the supports, while avoiding the complete filling of the pore spaces that was observed in the hyper branched or dendronized aminosilica adsorbents.[20] The adsorbents exhibit fast CO_2 adsorption−desorption kinetics, outstanding adsorption capacity, as well as good stability over multiple adsorption−desorption cycles. The structural characteristics and morphology of the novel macroporous adsorbents were evaluated by means of FTIR, ^{13}C NMR, EA, XRD, Brunauer−Emmett−Teller (BET) measurements, Hg porosimetry, SEM, and TEM. A detailed research on the CO_2 adsorptive behavior of these solid adsorbents was made based on thermogravimetric analysis (TGA).

EXPERIMENTAL SECTION

Materials. Monodispersed sulfonated polystyrene latex (PS, 2.62% solid latex, diameter 526 nm ± 18 nm) was bought from Polysciences. Tetraethoxysilane (TEOS, 99.0%), 3-aminopropyltri methoxysilane (APTMS, 97%), triphosgene (98%) and L-alanine (LA, 98%) were purchased from Sigma. All of these chemicals were used without additional purification.

Synthesis of Macroporous Silica Support. In a typical preparation process of macroporous silica, 550 mg of TEOS was added to a 10 mL of vial. Then 6.85 mL of PS suspension (526 nm) and 45 μL of nitric acid (70%) were dropped into the vial. The resulting mixture was continuously sonicated for 2 h, followed by centrifugation at 7000 rpm for 40 min. After drying at R.T. overnight, the PS templates were removed by calcination at 600 °C for 8 h with a heating rate of 2 °C/min.

Preparation of Macroporous Silica-Supported Amine Adsorbents. NCA of L-alanine was synthesized in dry THF from triphosgene and L-alanine using the reported procedure of Daly and Poche.[26] Amine-functionalized macroporous silica was prepared by postsynthetic grafting using 3-aminopropyltrimethoxysilane (APTMS). All reagents were handled under an inert atmosphere. Typically, 0.5 g of silica support was heated and dried under vacuum overnight at 100 °C. Then 30 mL of dry toluene followed by APTMS (0.375 mmol) were added. The resulting mixture was stirred constantly at room temperature for 24 h. Finally, the solid products were washed successively with toluene, methanol, methanol/water, and methanol, and finally dried in vacuum.

The PA was synthesized using the amines on the silica surface as initiators according to the previous report[23,27] with minor modification. Typically, A 0.2 M NCA of L-alanine solution was prepared in dry THF, and 56 mL (30:1 monomer/initiator), 112 mL (60:1 monomer/initiator), 168 mL (90:1 monomer/initiator), or 224 mL (120:1 monomer/initiator) of it were added to a 250 mL round-bottom flask containing 0.5 g of dried APTMS/g SiO_2 substrates. The resulting mixture was heated and vigorously stirred at 50 °C for 48 h. After completion, the powder was centrifuged and rinsed in 50 mL of THF, DMF, and chloroform. The composite was dried in a 40 °C oven and stored. The as-prepared adsorbents were denoted as MPS-LA-X, where X denotes the ratio of the monomer/initiator.

CO_2 Capture and Regeneration of the Adsorbents. CO_2 adsorption measurements under anhydrous conditions were performed using a Cahn 121 thermogravimetric analyzer using 10% CO_2 or 400 ppm CO_2 (balanced with argon). First, about 25 mg of the adsorbent was loaded to a platinum pan and subjected to pretreatment under argon atmosphere at 110 °C for 3 h with a heating rate of 10 °C min^{-1} to remove all the moisture and CO_2 adsorbed from the air. Then, the temperature was lowered to 25 °C (50 or 75 °C) with a rate of 10 °C min^{-1} and held for 60 min to stabilize the sample weight and temperature before introducing CO_2 containing gas. Adsorption experiments started after exposing the samples to a dry CO_2/Ar mixture for 90 min (10% CO_2) or 6 h (400 ppm CO_2). These adsorption times are long enough to attain (pseudo) equilibrium capacity as the weight change was lower than 0.002 mg min^{-1}. The adsorption enthalpies were calculated based on DSC heatflow profiles.

For the temperature swing, 25 mg sorbent was first exposed to 10% CO_2 (balanced with argon) at 50 °C for 40 min. The gas was then switched from CO_2 to pure Ar (25 mL min^{-1}) and the temperature was increased to 110 °C at a rate of 20 °C min^{-1} and held at that temperature for 10 min to regenerate the adsorbent.

Characterization. Scanning electron microscope (SEM) studies were carried out on a field-emission scanning electron microscope (SEM, Hitachi-4700). A JEOL 100CX transmission electron microscope was used to observe the particle morphology. Elemental analysis was carried out with Flash EA1112 (Thermo Finnigan Inc. Italy) for amine content of the MPS-supported amine adsorbents. The conformation of PA on silica was evaluated by FT-IR measurements with attenuated total reflection (ATR) method. IR spectra were obtained using 32 scans at a resolution of 4.0 cm^{-1} with a Spectrum One spectrometer attached ATR accessory (Perkin-Elmer, Japan). XRD patterns were obtained on a Scintag diffractometer using CuKα (λ = 1.54 Å) radiation. Solid-state ^{13}C NMR spectra were obtained using a Bruker DSX300 instrument equipped with double-bearing probes for cross-polarization (CP) and magic angle spinning (MAS). The resonance frequency for ^{13}C was 50 MHz, the sample was spun at the magic angle with a speed of 6.0 kHz. Inversely gated ^{13}C NMR spectra of PA cleaved from the MPS material were obtained in D_2O following literature methods.[28] For the cleaved polymer, a single drop of $Cr(acac)_2$ (where acac is acetylacetonate) was added to deuterated dimethylsulfoxide (DMSO) to aid relaxation and minimize interference from possible residual silica or base salts.

The Brunauer−Emmett−Teller (BET) surface area of dried samples was analyzed by nitrogen adsorption in a Micromeritics ASAP 2020 nitrogen adsorption apparatus using the adsorption data in the relative pressure (P/P_0) range of 0.05−0.3. The nitrogen adsorption volume at the relative pressure (P/P_0) of 0.99 was used to determine the pore volume. The desorption isotherm was used to determine the pore size distribution via the Barret−Joyner−Halender (BJH) method. All samples were degassed before nitrogen adsorption measurements. Hg intrusion and extrusion experiments were performed over a wide range for pressures starting in a vacuum up to 60000 psi with a Poremaster 60 instrument (Quantachrome Instruments, Boynton Beach, FL, USA). The pore size range assessed ranged from larger than 400 μm down to 4 nm. The amine loadings were determined by TGA using a Cahn thermogravimetric analyzer (TGA, Cahn model 121). Total organic loading was estimated as the weight loss from 150 to 750 °C, followed by inference of a stoichiometric ratio of L-alanine units (molecular weight of 71.1 Da) after accounting for silica surface silanol condensation. To estimate the molecular weights of PA grafted on silica support, The PA polymer was cleaved from the silica support by alkali treatment. Typically, the as-prepared adsorbent (~0.5 g) was dispersed in 100 mL of D.I. water. Then, 35 g of potassium hydroxide was added to the solution. The resulting mixture was stirred at 40 °C for 24 h. Then, the silica support was degraded into soluble species. The water was removed by evaporation at ~60 °C and the solution left was kept in a freezer overnight. Molecular weights of cleaved PAs from the silica were determined by aqueous size exclusion chromatography (ASEC) at 30 °C. The mobile phase consisted of 0.5 M acetic acid and 0.3 M Na_2SO_4, and the flow rate was maintained at 0.5 mL min^{-1}. Poly (ethylene glycol) narrow standards were used to calibrate the ASEC by the universal calibration method.

Scheme 1. Schematic Illustration of the Strategy and Motivation of Synthesis of 3D MPS-Supported Amine Adsorbent

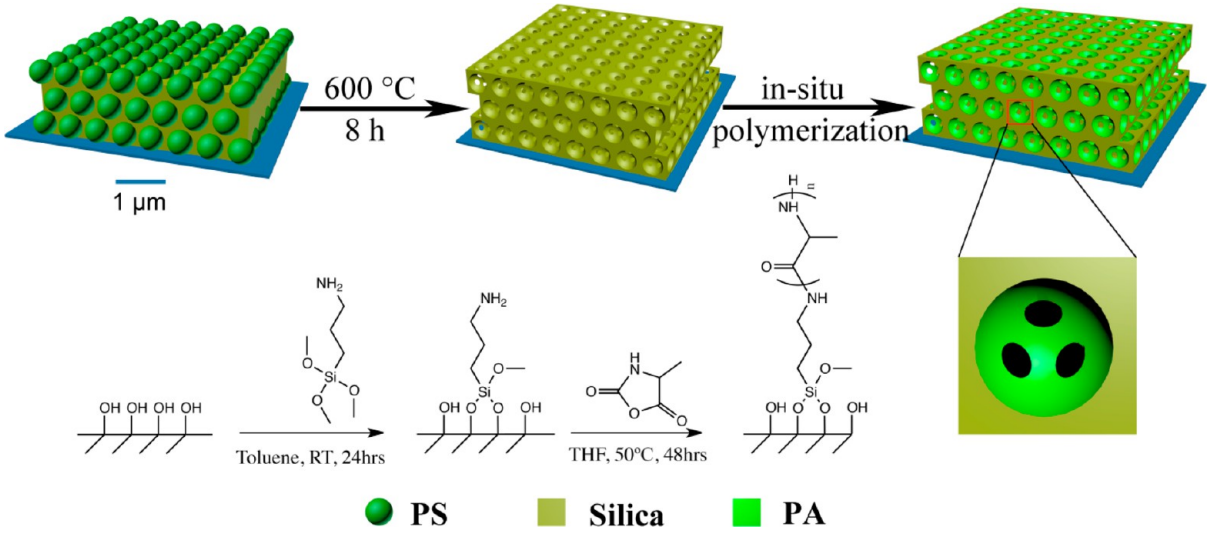

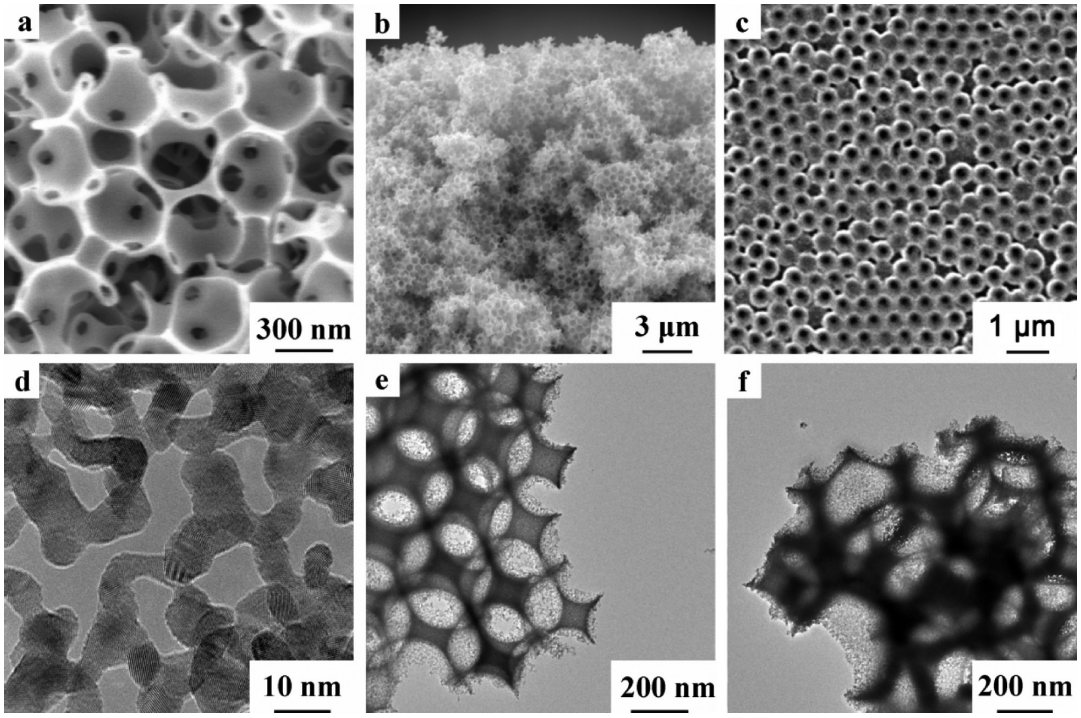

Figure 1. Morphologies of the representative MPS support and the composite adsorbents. (a) Top-down SEM image of the spongelike silica prepared from 526 nm sulfonated PS spheres. (b) Cross-sectional SEM image showing that the porous morphology is omnipresent in the matrix. (c) Cross-sectional SEM image of porous silica using a more concentrated silicon precursor solution (1.7 times greater than the one in b). (d) HRTEM image of the porous silica shell. (e) TEM image of macroporous silica before coating of PA. (f) TEM image of MPS-LA-60 after the coating of PA.

RESULTS AND DISCUSSION

Synthesis and Characterization of MPS-Supported Amine Adsorbents. An overall schematic depiction of the synthetic procedures for macroporous silica-supported amine adsorbent is shown in Scheme 1. The fabrication method of MPS support is inspired by evaporation-induced self-assembly technique (EISA) considered as an efficient structure-generating approach for nanocomposite materials.[29] In general, monodispersed hollow silica spheres will be obtained when the reported methods are followed which involve multiple steps including the formation of polystyrene (PS) latex templates, infiltration of precursor solution, and hydrolysis followed by calcination.[30,31] Here, we employed a facile one-pot procedure to direct the morphology of the silica toward monodispersed sponge-like macroporous matrix by controlling the surface charge of the polystyrene (PS) spheres and hydrolysis rates of the precursors. Sulfonated PS spheres are selected because the electrostatic repulsion between the charged PS particles ensures that they remain separated so that they can be fully surrounded by the precursor gel.[25,32] When an appropriate quantity of nitric acid is added, the pH is much less than 2, the increasing $[H^+]$ in solution neutralize the surface negative charge of sulfonated PS beads (reducing zeta potential) and also slow down the rate of hydrolysis. As such, the resulting structure contains a silicon gel

dx.doi.org/10.1021/am500089g | ACS Appl. Mater. Interfaces 2014, 6, 4371−4381

matrix material, which is distributed uniformly in the interstitial spaces of the PS opal spheres. As shown in Figure 1, upon firing, the silicon gel matrix yields an interconnected macropore matrix extending in all three spatial dimensions. Figure 1a is the high-magnification SEM image of the top layer of the macroporous silica using 526 nm PS beads as the sacrificial template and Figure S1in the Supporting Information shows the SEM image with a large field of view. The cross-sectional SEM image (Figure 1b) confirms that such an interconnected porous morphology is omnipresent in the matrix. The diameter of the pores on this top layer is ~391 nm and the wall thickness between each macropore on the top layer is ~43 nm. We estimate the calcination-induced shrinkage of the structure (the macropore diameter compared to that of the original PS spheres) to be about 25.7%. Such shrinkage is likely due to the loss of liquid volume within the precursor.[33] The disordered macropores in the top layer of the 3D structure connect the corresponding pores in the sublayer through the necks/joints ranging between 45−320 nm. These nanopores in the sublayer originate from the contact area between the PS spheres, which cannot be filled with the precursor material.[25] The pore density and wall thickness can be easily tailored by controlling the concentration of the silicon precursor because the slowed hydrolysis rate of the precursor can provide enough time for more infiltration of precursor into the interstitials. This was verified by a tougher 3D macroporous structure with a lower pore density and thicker wall prepared from a concentration of 1.7 times greater than the original precursor (Figure 1c). The HRTEM image (Figure 1d) shows that the porous shells are composed of nanocrystallites with a size of a few nanometers only. MPS-supported amine adsorbents for CO_2 capture were prepared by functionalization of silica support followed by in situ polymerization of NCA of L-alanine according to the previous report.[23,27] The as-prepared adsorbents were denoted as MPS-LA-X, where X denotes the ratio of the monomer/initiator. Scheme 1 summarizes the preparation procedure of the functionalization and in situ polymerization. Figure 1e shows the TEM image of macroporous silica before PA polymerization. Interestingly, the 3D interconnected framework is kept almost unchanged after the polymerization of PA (Figure 1f), whereas the surfaces become rather rough, indicating the successful in situ polymerization of PA. Furthermore, The IR spectra of MPS-supported amine adsorbents are shown in Figure S2 in the Supporting Information. An amide I absorption at 1633 cm^{-1} with a shoulder at 1655 cm^{-1} and an amide II absorption at 1540 cm^{-1} are observed, indicating that the PA moiety is mainly immobilized in a β -form structure.[23,34] The structures of the MPS-supported amine adsorbents are further confirmed by inversely gated ^{13}C NMR spectra of PA cleaved from the MPS material. As shown in Figure S3 in the Supporting Information, three intense peaks at 172.1, 49.5, and 19.9 ppm can be assigned to the C═O, C_α, and C_β carbons of the PA, respectively, which are in agreement with the values reported before.[35]

Solid ^{13}C CP MAS NMR spectra for the adsorbent before and after contact with CO_2 are presented in Figure 2. The three intense peaks at 172.3, 49.4, and 20.2 ppm can be assigned to the C═O, C_α, and C_β carbons, respectively. The ^{13}C chemical shift values show that the PA used in this work takes the β-form structure,[36] which is consistent with the IR result. After exposure to CO_2, the peak at 164.5 ppm is assigned to the carbamate ions formed by reaction of CO_2 with the amine groups on the surface of the solid, already identified by other authors.[37]

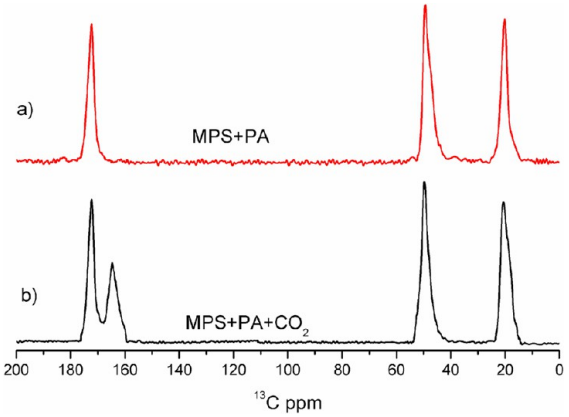

Figure 2. ^{13}C CPMAS NMR spectra of (a) MPS + PA without CO_2, and (b) MPS + PA with CO_2.

Powder XRD patterns of the composite adsorbents show relatively broad diffraction peaks at 2θ of 2.50° (see Figure S4 in the Supporting Information). The similar peak positions suggest that the macroporous structure was retained after the in situ polymerization of L-alanine. However, the diffraction intensity of the amine-loaded silica decreases as the organic loading increases, suggesting the increasing filling of the interior pores with PA because the diffraction peak intensity is correlated with the scattering contrast between the silicate walls and the pores.[38,39]

The MPS-supported amine adsorbents fabricated in this study were characterized with N_2 adsorption and Hg intrusion to understand the pore structures. Hg intrusion is most sensitive to pores with diameters >20 nm, whereas the small size and gaseous delivery of N_2 atoms make their adsorption best suited to characterize mesopores and micropores.[40] The N_2 adsorption/desorption isotherms and the pore size distribution of the MPS-supported amine adsorbents are shown in Figure 3. The BET surface areas and total pore volumes were calculated to vary from 825 to 56 $m^2\ g^{-1}$ and from 0.89 to 0.11 $cm^3\ g^{-1}$, respectively, depending on the polyamine loadings (Table 1).

Figure 3a demonstrates a fundamental type II isotherm, which corresponds to macroporous structures. A type H3 hysteresis loop can also be identified around 1.0 P/P_0 due to the abundance of macropores. Furthermore, a type H3 loop is also highly likely to form a reliable pore size distribution (PSD) analysis. The PSD (Figure 3b) indicates that the silica support has a variety of nanopores in the range of 1−100 nm with a peak centered at ~19 nm. The BET surface areas and pore volumes decrease when the organic loadings increase, suggesting that the polyamines are formed in the interiors of the MPS support.[41−43] Interestingly, Figure 3b indicates that micropores and mesopores do not disappear in the MPS adsorbents until relatively high amine loadings are obtained. Even with a very high amine loading, MPS-LA-120 still possesses a pore volume of 0.11 $cm^3\ g^{-1}$.

Because the N_2 adsorption measurements cannot capture pore sizes that are much larger than 20 nm, it was complemented by Hg porosimetry. Pore size distributions for all MPS-supported amine adsorbents derived from Hg intrusion data (Figure 4a) are shown in Figure 4b. All textural parameters from Hg intrusion are presented in Table 1. The pore

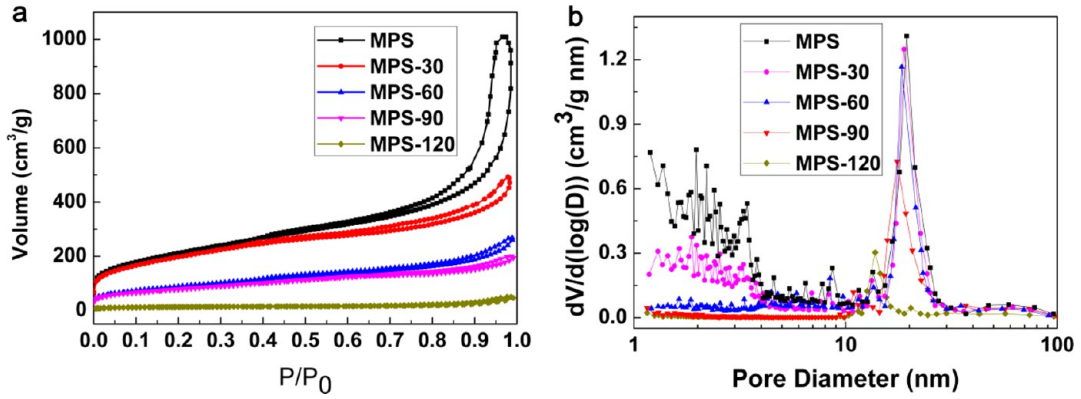

Figure 3. (a) Nitrogen adsorption/desorption isotherms of MPS-supported amine adsorbents, and (b) pore size distribution calculated from the desorption branch.

Table 1. Structural Features of the MPS Support and the Composite Adsorbents Calculated from N_2 Adsorption and Hg Intrusion Data

sample	N_2 adsorption BET surface area (m^2 g^{-1})	N_2 adsorption pore volume (cm^3 g^{-1})	Hg intrusion surface area (m^2 g^{-1})	Hg intrusion pore volume (cm^3 g^{-1})	Hg intrusion apparent density (g^{-1} cm^3)
MPS	825	0.89	571	4.02	1.043
MPS-LA-30	517	0.83	339	3.13	1.062
MPS-LA-60	322	0.57	212	2.93	1.089
MPS-LA-90	169	0.19	119	2.58	1.099
MPS-LA-120	56	0.11	42	2.01	1.093

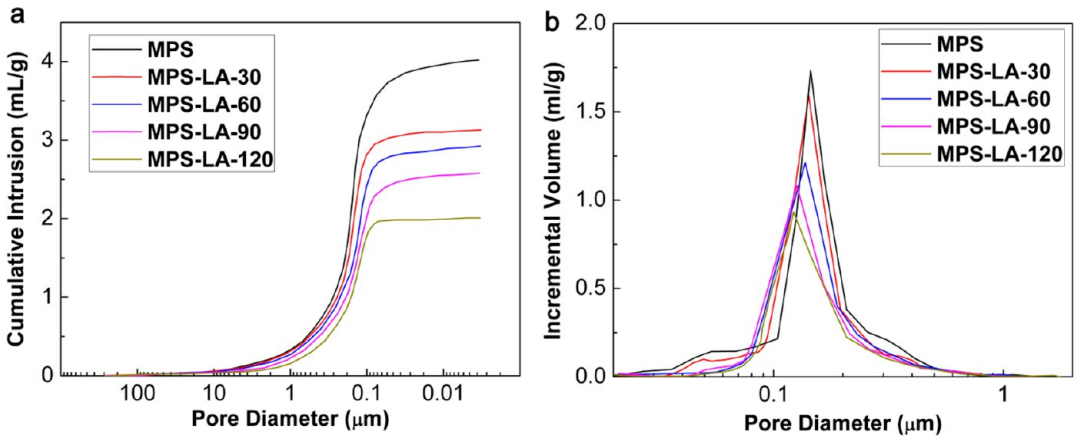

Figure 4. (a) Hg cumulative intrusion, and (b) Hg intrusion pore size distributions versus pore diameter data of all MPS-supported amine adsorbents. The volume of the big pores is measured as the volume belonging to the pore size of the pore entrance.

Table 2. Amine Loading of Cleaved PA and Calculated Molecular Weights and Repeat Units

sample	monomer/initiator ratio	amine loading (mmol N g^{-1})[a]	amine loading (mmol N g^{-1})[b]	avg M_w (Daltons)	avg. repeat units
MPS-LA-30	30	3.02	~3.11	4281	~59
MPS-LA-60	60	6.45	~6.57	8370	~117
MPS-LA-90	90	8.79	~8.92	11833	~164
MPS-LA-120	120	10.98	~11.03	13058	~183

[a]Values were determined from elemental analysis. [b]Values were calculated from TGA.

diameters decrease from 143 nm for MPS to 119 nm for MPS-LA-120. As observed from the N_2 adsorption/desorption isotherms, the surface areas and pore volumes decrease when the organic loadings increase. These pores are much smaller than those observed in SEM because Hg intrusion measures the smallest openings between pores.[40] So, the volume of the big pores is measured as the volume belonging to the pore size of the pore entrance. These openings are the macropore windows seen in Figure 1a, and the macropore windows observed in SEM images are in good agreement with the Hg intrusion data.

dx.doi.org/10.1021/am500089g | ACS Appl. Mater. Interfaces 2014, 6, 4371−4381

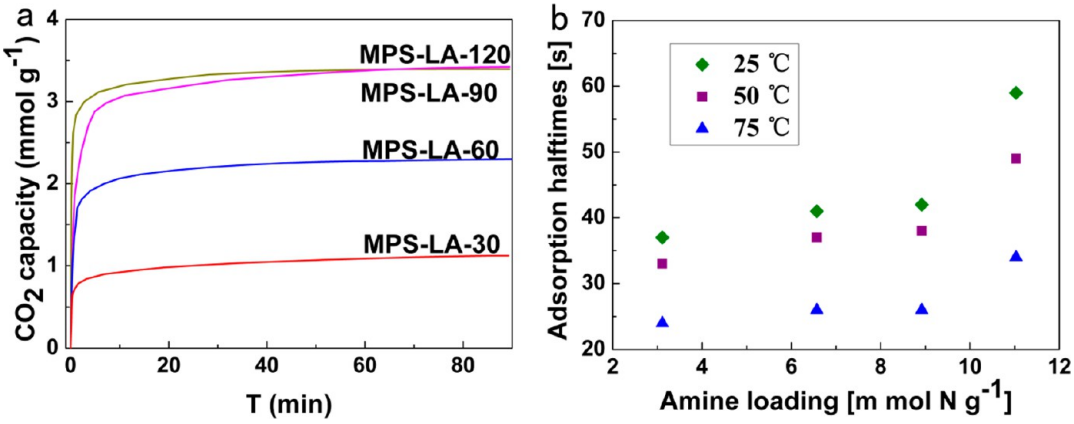

Figure 5. (a) CO_2 capture kinetics of MPS-supported amine adsorbents in 10% CO_2 at 25 °C. (b) Adsorption halftimes of the MPS-supported amine adsorbents in 10% CO_2 at operating temperatures of 25, 50, and 75 °C.

This hierarchically multimodal pore size distribution, which combines the benefits of high surface area of micropores and mesoporosity and the accessible diffusion pathways of macroporous networks, is assigned to the porous shell and the interconnected macropores formed by the sacrificial PS beads.

The degree of polymerization of PA on the MPS was evaluated. The supported PA was cleaved from the supports by dissolution of the silica framework in concentrated alkali solution using the reported procedure.[11,20] The molecular weights of the cleaved polyamines were determined by aqueous size exclusion chromatography (ASEC, Figure S5 in the Supporting Information). A continuous shift of the curves toward smaller retention times is observed, indicating continuous increase of molecular weights. The amine loadings were determined by elemental analysis (Table 2). We also estimated the amine loadings by total organic loading weight loss from 150 to 750 °C (see Figure S6 in the Supporting Information), followed by inference of a stoichiometric ratio of L-alanine units after accounting for silica surface silanol condensation. As shown in Table 2, when the monomer/initiator ratio is increased from 30 to 90, the amine loading obtained increases in a roughly linear fashion. When the monomer/initiator ratio is 120, the average molecular weight is as high as 13058 with a high amine loading of 10.98 mmol N g^{-1}, which will greatly increases the accessible adsorption sites in the adsorbent. To the best of our knowledge, this adsorbent has the highest molecular weight and amine loading among the chemically tethered amine adsorbents that have been ever prepared. Lunn et al.[23] found that mesopores provide confinement effects that decrease the final molecular weight. So, the high molecular weights and amine loadings can be assigned to the macropores that can provide more free space for the growth of the polymer chains, whereas prevent the clogging and maintain the porosity of the adsorbents after the in situ polymerization.

CO_2 Capture Kinetics. For capturing CO_2 from the flue gas in a practical way, the adsorbent should adsorb and desorb CO_2 as fast as possible.[20] The CO_2 adsorption capacity and the rate of CO_2 adsorption of these MPS-supported amine adsorbents at 25 °C are shown in Figure 5. A maximum adsorption rate appears in the first ~1−2 min when CO_2 gas is introduced. Except MPS-LA-120, the conversion of all the other three adsorbents reaches as high as 90% within ~5 min. The adsorption rates are comparable to those of amine-functionalized mesoporous adsorbents reported before, *i.e.* 83% of the equilibrium CO_2 capacity was reached in 1 min for AMS-6/APMDES reported by Bacsik et al.[44] Yang determined that 80% of its equilibrium capacity was reached after 30 min for 3-aminopropyl-functionalized MCM-48 sample under dry conditions.[45] For other amine-functionalized porous materials, Measurements by Pis indicated that amine-impregnated activated carbons reached equilibrium in approximately 40 min.[46] Endo determined that styrene and DBN copolymers did not reach equilibrium for hundreds of minutes.[47] It was reported that the pore channels of the mesoporous silica-supported adsorbents are significantly constricted and even blocked when a large amount of amines are loaded. In addition, the amino groups may be unevenly distributed in the mesoporous materials.[18,19] As a result, the pressure resistance increases substantially as the free spaces between mesoporous particles are filled with amine molecules, and finally slows down the kinetics. Two reasons lie behind the fast adsorption and desorption kinetics of the MPS-supported adsorbents. One is the linear polymer structure can avoid the complete filling of the pore spaces, which was observed in the hyper branched or dendronized aminosilica adsorbents.[48] The other is attributed to the 3D interconnected macroporous structure that provides low resistant pathways for the diffusion of CO_2 molecules. The adsorption curves shown in Figure 5a also indicate that the CO_2 uptake into PA in macroporous adsorbents takes place in two stages. The fast surface chemical reaction with a sharp linear weight gain dominates the beginning stage and is followed by a relatively slow diffusion stage.[49] In the first surface adsorption stage, the uptake rate is controlled by the fast chemical reaction between CO_2 and amines. Thereafter, the uptake rate is slowed down because of the slowly diffusion of the CO_2 into the lower PA multilayers in the second stage. As verified in Figure 5b, the adsorption and desorption kinetics are accelerated by increasing the temperature from 25 to 75 °C.[38] Figure 5b also shows the adsorption halftimes (the time where the adsorbent reaches half of its capacity at the end of the experiment) of these as-synthesized adsorbents range from 20 to 60 s. Similar adsorption kinetics also have been observed in covalently tethered amine adsorbents.[23,27,41,50] Because of the mass transfer limitations, a higher organic content also results in slower adsorption kinetics as reflected by increased adsorption half times.

CO_2 Adsorption Capacities. The DSC heatflow profiles during adsorption process are given in Figure S7 in the Supporting Information, and the adsorption enthalpies of

Table 3. CO_2 Adsorption Characteristics of Composite Adsorbents under Dry Conditions Using Simulated Flue Gas (10% CO_2) at Different Temperatures

		capacity (mmol CO_2 g^{-1})			amine efficiency (mol CO_2 N^{1-})			
sample	amine loading (mmol N g^{-1})	25 °C	50 °C	75 °C	25 °C	50 °C	75 °C	adsorption enthalpies (kJ/mol)[a]
MPS-LA-30	3.02	1.12	1.18	1.03	0.36	0.38	0.33	61
MPS-LA-60	6.45	2.30	2.43	1.90	0.35	0.37	0.29	63
MPS-LA-90	8.79	3.39	3.66	2.68	0.38	0.41	0.30	67
MPS-LA-120	10.98	3.42	3.86	2.76	0.31	0.35	0.25	68

[a]Adsorption at 50 °C.

adsorbents integrated from the DSC heatflow profiles are shown in Table 3. It can been seen from Table 3 that the calculated values of adsorption enthalpies are all above 60 kJ/mol which are in the range of the enthalpy of chemical sorption, suggesting that the adsorption interactions between CO_2 and the MPS-supported amine adsorbents are strong.

CO_2 capture capacities of the hybrid adsorbents were evaluated by TGA under dry conditions using simulated flue gas (10% CO_2 balanced with argon). The capture capacities and amine efficiencies at different temperatures are summarized in Table 3. It was reported that the temperature dependency is almost always the case when mesoporous supports are used and the amines are physically adsorbed (impregnation).[38] However, we show here an unusual temperature dependency of the maximal CO_2 uptake when covalently amines are tethered. As shown in Table 3, as temperature increases, the CO_2 adsorption capacity increases with increasing temperature up to 50 °C. This behavior is associated with the diffusion-controlled process, which is consistent with the fact that the pores have been filled with PA, thus limiting the accessibility of amine sites. So, although the adsorption of CO_2 into the adsorbents is an exothermic process (Table 3), as the temperature increases up to 50 °C, the CO_2 adsorption capacity increases as a result of diminished diffusion resistance.[38] Table 3 also shows that the temperature dependency increases when the amine loading increases from MPS-LA-30 to MPS-LA-120. So, the limited diffusion may be due, in part, to the polymers with high molecular weights than the structure of the silica support since all the samples have the same macroporous structure. Beyond 50 °C, CO_2 diffusion becomes faster than CO_2 adsorption, the equilibrium is achieved and the adsorption capacity decreases as expected. As such, the adsorption capacity reaches a maximum near 50 °C, because of the competition between the exothermic adsorption reaction and the diffusion kinetics.

The adsorption capacity of CO_2 increases with the increase of the amine loading. The maximum adsorption capacities in 10% dry CO_2 at temperatures of 25, 50, and 75 °C are 3.42, 3.86, and 2.76 mmol CO_2 g^{-1}, respectively (Figure 6), which are among the best behaved covalently tethered adsorbents. For example, Hicks et al. prepared HAS material which is capable of adsorbing CO_2 reversibly with very high capacity of 3.1 mmol CO_2 g^{-1} material at 25 °C.[11] Drese et al. synthesized hyperbranched aminosilica adsorbents via the ring-opening polymerization of aziridine in the presence of mesoporous silica SBA-15 support with the highest capacity of 5.55 mmol CO_2 g^{-1} under humid condition.[20] Chaikittisilp et al. prepared the poly (L-lysine) brush−mesoporous silica hybrids with capacity of 1.15 mmol CO_2 g^{-1} material in 10% dry CO_2.[27] Several groups also have investigated other porous amide-functionalized materials, i.e. Barron measured CO_2 capacities of 0.93, 1.09, 1.18, and 1.64 mmol CO_2 g^{-1} for SWNTs functionalized with PEI of different molecular weights (600, 1800, 10000, 25000) by TGA at 348 K.[51] Pis determined capacities of 0.91, 1.09, and 1.11 mmol CO_2 g^{-1} for DETA, PEHA, and PEI impregnated commercial activated carbon.[46] The high adsorption capacity is ascribed to the improved adsorption sites per weight/volume unit of the adsorbent.[43,52] The amine efficiency (the amount of CO_2 captured divided by the amount of amines present for a given weight of adsorbent) of the MPS-supported amine adsorbents at different temperatures is shown in Figure 6. At low loadings, the amine efficiency is almost constant. The maximum amine efficiency of 0.41 for MPS-LA-90 at 50 °C is among the highest values reported for chemically tethered amine adsorbents, i.e., 0.22 for poly(L-lysine) brush−mesoporous silica hybrids,[27] 0.44 for hyperbranched aminosilica prepared from aziridine with the presence of H_2O,[11] and 0.55 for bicontinuous mesoporous silica adsorbents modified with (3-aminopropyl)triethoxysilane,[44] The slight decrease in amine efficiency for MPS-LA-120 is probably due to the loss of pore volume and reduced mass transfer rate.[20] It was reported that two moles of primary amines and secondary amines react with one mole of CO_2 and lead to the formation of carbamate ion pairs as well as carbamic acid, and the uptake of CO_2 can be enhanced in the presence of water because of the release of additional amine groups.[44,53−57] So, it is expected that higher amine efficiency value could be attained in the presence of water vapor as compared with dry CO_2.

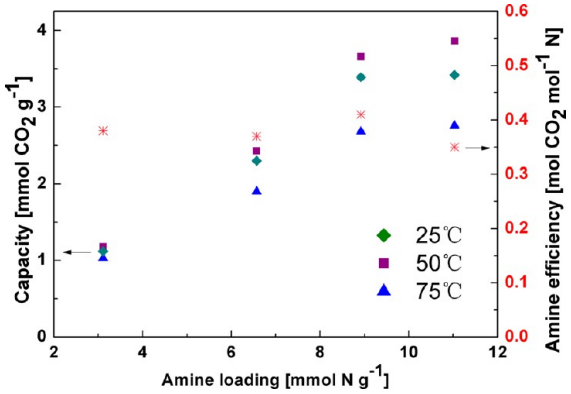

Figure 6. CO_2 capture capacities of the adsorbents in 10% CO_2 at 25, 50, and 75 °C and associated amine efficiency at 50 °C versus amine loadings.

Stability of the Adsorbents. A crucial issue for amine-functionalized adsorbents is their chemical stability during the regeneration process, which comes from amine degradation induced by impurities of the flue gas such as SO_2.[58] Prior to absorption, acid gases such as SO_2 must be removed in a flue gas desulphurization (FGD) unit, because they will possibly foul the solid sorbent, which can lead to increased complexity, energy consumption, and costs. To reduce the cost of CO_2 capture, adsorbents must also be regenerable, enabling their use

in a large number of cycles. The adsorption processes for postcombustion CO_2 capture are usually based on temperature or pressure (vacuum) swing depending on the adsorbent properties. The nature of the adsorbent−adsorbate interactions plays a major role in establishing the appropriate driving force required for regeneration. In the case of pressure swing adsorption (PSA), the mass transfer kinetics and the shape of the isotherm are critical. If mass transfer is really fast, the adsorption capacity is not very important because it can be compensated by a faster cycling.[59] On the contrary, in the case of temperature swing adsorption (TSA), mass transfer kinetics is of secondary importance because the adsorber dimensions are governed by heat transfer. The critical parameters are the adsorption capacity per mass of solid (because it determines the parasitic heat loss) and the heat of adsorption, which expresses the temperature dependence of the adsorption capacity.[60,61] For these MPS-supported amine adsorbents, the adsorption capacity is as high as 3.86 mmol CO_2 g^{-1} in simulated flue gas under 1 atm of dry CO_2. Moreover, the CO_2-adsorbent interactions are chemical in nature (adsorption enthalpies are all above 60 kJ/mol, Table 3), which means there is a fair temperature dependence of the adsorption capacity, heat-driven regeneration mode (TSA) is more appropriate than PSA. In addition, as shown in Figure S6 in the Supporting Information, MPS-supported amine adsorbents at 110 °C are stable when regeneration mode is used. For these reasons, we have chosen to evaluate the potential of postcombustion capture by temperature swing adsorption (TSA).

The adsorbents were first exposed to the 10% dry CO_2 at 50 °C for 40 min to get an equilibrium adsorption. Then these samples were regenerated under Ar at 110 °C for 10 min. Figure 7 depicts the adsorption−desorption cycles of MPS-LA-90 and MPS-LA-120. The CO_2 capacity dropped only ∼2% after 120 cycles for both adsorbents. For adsorbents physically impregnated with monomeric or polymeric amines, the lack of chemical bonds between the support and the active adsorbent can result in amine leaching and limited stability in the regeneration process.[9] For example, Goeppert et al. showed that the fumed silica supported low molecular weight PEI (branched, M_w ca. 800) had an adsorption capacity of 147 mg g^{-1} at 70 °C, but it suffered from serious leaching similar to "oligomeric" ethyleneamines.[62] For other functionalized adsorbents, Gray measured a 20% decrease in capacity of amine-functionalized fly ash when regenerated at 393 K after one adsorption/desorption cycle,[63] whereas PEI and ECH copolymers were found by Chen to lose 6% capacity after one cycle at the same temperature.[64] The excellent cyclic performance of MPS-LA-90 and MPS-LA-120 can be assigned to the high boiling point of PA and the strong chemical bonds, which contribute to better temperature stability.

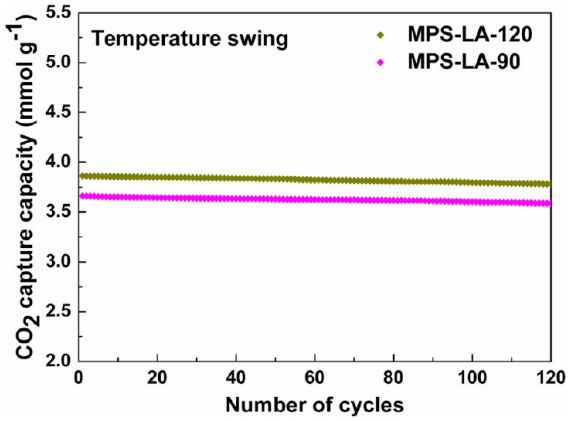

Figure 7. Temperature swing cyclic stability of MPS-LA-90 and MPS-LA-120. Adsorption in 10% CO_2 at 50 °C for 40 min and desorption at 110 °C for 10 min under 1 atm pure Ar.

The current state-of-the-art postcombustion capture technology is absorption of CO_2 by an aqueous monoethanolamine (MEA) solution. However, the regeneration of the solvent by heating requires a large amount of energy (from 20 to 40% energy penalty).[65] Moreover, degradation of the amine by O_2 or SO_2 in the flue gas causes corrosion problems and leads to a high net consumption of solvent (>1.4 kg MEA/t CO_2 captured, i.e., >4700 t per year for a 600 MW power plant).[59] Solid-supported amine adsorbents based on silica show fast CO_2 adsorption kinetics and enhanced capacity compared to those based on aqueous amine solutions. To the best of our knowledge, the highest capture capacities of the covalently tethered CO_2 solid sorbents were 5.55 mmol g^{-1} (under 1 atm humid condition)[20] and 2.65 mmol g^{-1} (under 1 atm dry condition),[66] respectively, whereas the MEA-rich solution is limited to about 45% molar load of CO_2 to MEA (2.2 mmol g^{-1} of solution).[67] Previous information indicates that capacity for the dry-sorbent processes is going to have to be generally above about 3 mmol g^{-1} to have a chance of providing energy reductions of 30−50% or more compared to the optimum aqueous-MEA-based processes.[67] Here, we prepared covalently tethered solid amine adsorbent with adsorption capacity of 3.8 mmol g^{-1} in simulated flue gas. This high adsorption capacity ensures the relatively low reaction heat compared to amine-scrubbing solvents such as 30% MEA solution, finally leading to less energy penalty for adsorbent regeneration. In perspective, these adsorbents are very promising new materials for acid gas capture from flue gas streams and are viable alternatives to the current state-of-the-art.

CO_2 Capture from the Air. Although CO_2 capture from concentrated sources such as fossil fuel burning power plants, natural sources and industrial plants followed by sequestration into geologic formation or under the seas has been the most practical to reduce the environmental harm, the capture of CO_2 from the atmosphere is also technically feasible despite its low concentration and presents even some benefits compared to point source CO_2 capture.[9,68] Hence we measured the CO_2 adsorption capacities of the MPS-supported amine adsorbents using simulated ambient air (400 ppm CO_2 balanced with Ar) under dry conditions at 50 °C. As shown in Table 4, the amine capacities increase with the increase of the amine loadings,

Table 4. Capture Capacities of Composite Adsorbents under Dry Conditions Using Simulated Ambient Air (400 ppm CO_2) at 50 °C

sample	amine loading (mmol N g^{-1})	capacity (mmol CO_2 g^{-1})	amine efficiency (mol CO_2 per mol N)
MPS-LA-30	3.02	0.78	0.25
MPS-LA-60	6.45	1.51	0.23
MPS-LA-90	8.79	2.05	0.23
MPS-LA-120	10.98	2.65	0.24

which is in agreement with the experiments using flue gas concentrations, while the amine efficiency is almost constant, suggesting that the ability to bind CO_2 at moderately low concentration is independent of the density of amine groups within the range investigated. A high amount of 2.65 mmol CO_2 g^{-1} adsorbent is observed for MPS-LA-120, which exhibits a decrease of CO_2 capture capacity by a factor of ca. 1.46 when the CO_2 concentration is reduced from 10% to 400 ppm. The maximum adsorption capacity of 2.65 mmol CO_2 g^{-1} adsorbent at 50 °C is comparable to or better than the reported chemically tethered amine adsorbents measured at a lower temperature of 25 °C,[41,69] i.e., 2.36 mmol g^{-1} for a class 1 aminosilica adsorbent, comprising PEI loaded into porous silica,[70] 0.60 mmol g^{-1} for the poly (L-lysine) brush−mesoporous silica hybrids,[27] 1.72 mmol g^{-1} for hyperbranched aminopolymers in porous silica supports.[41,69] The improved performance of these new MPS-supported amine adsorbents may be due to, in part, the elevated temperature used. These results suggest that the PA-hybrids can capture considerable amounts of CO_2 from ultradilute CO_2 sources, specifically at concentrations similar to those found in the ambient air, and thus can be promising amine adsorbents for CO_2 capture from ambient air.

CONCLUSIONS

In summary, we have synthesized and evaluated a new, highly efficient CO_2 amine adsorbent based on 3D interconnected macroporous silica. Under dry conditions, the best behaved adsorbent is capable of adsorbing CO_2 reversibly with very high capacities of 3.86 mmol CO_2 g^{-1} adsorbent in simulated flue gas and 2.65 mmol CO_2 g^{-1} adsorbent in simulated ambient air at 50 °C. The advantages of these adsorbents over previously reported adsorbents rest in their fast kinetics, large CO_2 capacity, and good stability over repetitive adsorption−desorption cycling due to the covalently attachment between the support and the organic groups. This study lays the groundwork for the future studies of MPS-supported amine adsorbents. New methods for the synthesis of the MPS supports using less expensive surfactant or polymer template need to be undertaken. Such studies are currently underway in our laboratory.

ASSOCIATED CONTENT

Supporting Information

SEM image, FT-IR spectra, inversely gated ^{13}C NMR spectrum, powder XRD patterns, plots of the retention time of the aqueous size exclusion chromatograms, TGA patterns, and DSC heatflow. This material is available free of charge via the Internet at http://pubs.acs.org.

AUTHOR INFORMATION

Corresponding Author

*E-mail: faqianliu@yahoo.com.

Notes

The authors declare no competing financial interest.

ACKNOWLEDGMENTS

This work was supported by the NSF of China (21371105 and 51372125), the NSF of Shandong Province (2009ZRA02071), the Scientific Development Plan of University in Shandong Province (J09LB53), and the Doctoral Science Foundation of QUST.

REFERENCES

(1) Conway, W.; Wang, X. G.; Fernandes, D.; Burns, R.; Lawrance, G.; Puxty, G.; Maeder, M. Toward the Understanding of Chemical Absorption Processes for Post-Combustion Capture of Carbon Dioxide: Electronic and Steric Considerations from the Kinetics of Reactions of CO_2(aq) with Sterically hindered Amines. *Environ. Sci. Technol.* **2013**, *47*, 1163−1169.

(2) Wang, Q. A.; Luo, J. Z.; Zhong, Z. Y.; Borgna, A. CO_2 Capture by Solid Adsorbents and Their Applications: Current Status and New Trends. *Energy Environ. Sci.* **2011**, *4*, 42−55.

(3) Yang, Z. Z.; He, L. N.; Gao, J.; Liu, A. H.; Yu, B. Carbon Dioxide Utilization With C−N Bond Formation: Carbon Dioxide Capture and Subsequent Conversion. *Energy Environ. Sci.* **2012**, *5*, 6602−6639.

(4) Goeppert, A.; Meth, S.; Prakash, G. K. S.; Olah, G. A. Nanostructured Silica As a Support for Regenerable High-Capacity Organoamine-Based CO_2 Sorbents. *Energy Environ. Sci.* **2010**, *3*, 1949−1960.

(5) Rinker, E. B.; Ashour, S. S.; Sandall, O. C. Absorption of Carbon Dioxide into Aqueous Blends of Diethanolamine and Methyldiethanolamine. *Ind. Eng. Chem. Res.* **2000**, *39*, 4346−4356.

(6) Franchi, R. S.; Harlick, P. J. E.; Sayari, A. Applications of Pore-Expanded Mesoporous Silica. 2. Development of a High-Capacity, Water-Tolerant Adsorbent for CO_2. *Ind. Eng. Chem. Res.* **2005**, *44*, 8007−8013.

(7) Choi, S.; Drese, J. H.; Jones, C. W. Adsorbent Materials for Carbon Dioxide Capture from Large Anthropogenic Point Sources. *Chemsuschem* **2009**, *2*, 796−854.

(8) Zhao, J. Q.; Simeon, F.; Wang, Y. J.; Luo, G. S.; Hatton, T. A. Polyethylenimine-Impregnated Siliceous Mesocellular Foam Particles As High Capacity CO_2 Adsorbents. *RSC Adv.* **2012**, *2*, 6509−6519.

(9) Goeppert, A.; Czaun, M.; Prakash, G. K. S.; Olah, G. A. Air as the Renewable Carbon Source of the Future: An Overview of CO_2 Capture from the Atmosphere. *Energy Environ. Sci.* **2012**, *5*, 7833−7853.

(10) Hao, G. P.; Li, W. C.; Lu, A. H. Novel Porous Solids for Carbon Dioxide Capture. *J. Mater. Chem.* **2011**, *21*, 6447−6451.

(11) Hicks, J. C.; Drese, J. H.; Fauth, D. J.; Gray, M. L.; Qi, G. G.; Jones, C. W. Designing Adsorbents for CO_2 Capture from Flue Gas-Hyperbranched Aminosilicas Capable,of Capturing CO_2 Reversibly. *J. Am. Chem. Soc.* **2008**, *130*, 2902−2903.

(12) Bollini, P.; Didas, S. A.; Jones, C. W. Amine-Oxide Hybrid Materials for Acid Gas Separations. *J. Mater. Chem.* **2011**, *21*, 15100−15120.

(13) Li, W.; Bollini, P.; Didas, S. A.; Choi, S.; Drese, J. H.; Jones, C. W. Structural Changes of Silica Mesocellular Foam Supported Amine-Functionalized CO_2 Adsorbents Upon Exposure to Steam. *ACS Appl. Mater. Interfaces* **2010**, *2*, 3363−3372.

(14) Li, W.; Choi, S.; Drese, J. H.; Hornbostel, M.; Krishnan, G.; Eisenberger, P. M.; Jones, C. W. Steam-Stripping for Regeneration of Supported Amine-Based CO_2 Adsorbents. *Chemsuschem* **2010**, *3*, 899−903.

(15) Harlick, P. J. E.; Sayari, A. Applications of Pore-Expanded Mesoporous Silica. 5. Triamine Grafted Material with Exceptional CO_2 Dynamic and Equilibrium Adsorption Performance. *Ind. Eng. Chem. Res.* **2007**, *46*, 446−458.

(16) Gerardin, C.; Reboul, J.; Bonne, M.; Lebeau, B. Ecodesign of Ordered Mesoporous Silica Materials. *Chem. Soc. Rev.* **2013**.

(17) Liu, Y.; Goebl, J.; Yin, Y. Templated Synthesis of Nanostructured Materials. *Chem. Soc. Rev.* **2013**, *42*, 2610−53.

(18) Yue, M. B.; Sun, L. B.; Cao, Y.; Wang, Y.; Wang, Z. J.; Zhu, J. H. Efficient CO_2 Capturer Derived from As-Synthesized MCM-41 Modified with Amine. *Chem.—Eur. J.* **2008**, *14*, 3442−3451.

(19) Yue, M. B.; Chun, Y.; Cao, Y.; Dong, X.; Zhu, J. H. CO_2 Capture by As-Prepared SBA-15 with an Occluded Organic Template. *Adv. Funct. Mater.* **2006**, *16*, 1717−1722.

(20) Drese, J. H.; Choi, S.; Lively, R. P.; Koros, W. J.; Fauth, D. J.; Gray, M. L.; Jones, C. W. Synthesis-Structure-Property Relationships for Hyperbranched Aminosilica CO_2 Adsorbents. *Adv. Funct. Mater.* **2009**, *19*, 3821−3832.

(21) Hiyoshi, N.; Yogo, K.; Yashima, T. Adsorption of Carbon Dioxide on Amine Modified SBA-15 in the Presence of Water Vapor. *Chem. Lett.* **2004**, *33*, 510−511.
(22) Bollini, P.; Brunelli, N. A.; Didas, S. A.; Jones, C. W. Dynamics of CO_2 Adsorption on Amine Adsorbents. 2. Insights Into Adsorbent Design. *Ind. Eng. Chem. Res.* **2012**, *51*, 15153−15162.
(23) Lunn, J. D.; Shantz, D. F. Peptide Brush-Ordered Mesoporous Silica Nanocomposite Materials. *Chem. Mater.* **2009**, *21*, 3638−3648.
(24) Liu, F.-Q.; Li, W.-H.; Liu, B.-C.; Li, R.-X. Synthesis, Characterization, and High Temperature CO_2 Capture of New CaO-Based Hollow Sphere Sorbents. *J. Mater. Chem. A* **2013**, *1*, 8037−8044.
(25) Liu, F.-Q.; Wu, H.; Li, T.; Grabstanowicz, L. R.; Amine, K.; Xu, T. Three-dimensional conducting oxide nanoarchitectures: morphology-controllable synthesis, characterization, and applications in lithium-ion batteries. *Nanoscale* **2013**, *5*, 6422−6429.
(26) Daly, W. H.; Poche, D. The Preparation of N-Carboxyanhydrides of Alpha-Amino-Acids Using Bis(Trichloromethyl)Carbonate. *Tetrahedron Lett.* **1988**, *29*, 5859−5862.
(27) Chaikittisilp, W.; Lunn, J. D.; Shantz, D. F.; Jones, C. W. Poly(L-lysine) Brush-Mesoporous Silica Hybrid Material as a Biomolecule-Based Adsorbent for CO_2 Capture from Simulated Flue Gas and Air. *Chem.—Eur. J.* **2011**, *17*, 10556−10561.
(28) Pierre, T. S.; Geckle, M. ^{13}NMR Analysis of Branched Polyethyleneimine. *J. Macromol. Sci., Chem.* **1985**, *22*, 877−887.
(29) Brinker, C. J.; Lu, Y. F.; Sellinger, A.; Fan, H. Y. Evaporation-induced self-assembly: Nanostructures made easy. *Adv. Mater.* **1999**, *11*, 579−585.
(30) Qi, G. G.; Wang, Y. B.; Estevez, L.; Duan, X. N.; Anako, N.; Park, A. H. A.; Li, W.; Jones, C. W.; Giannelis, E. P. High efficiency nanocomposite sorbents for CO_2 capture based on amine-functionalized mesoporous capsules. *Energy Environ. Sci.* **2011**, *4*, 444−452.
(31) Zhang, L.; D'Acunzi, M.; Kappl, M.; Auernhammer, G. K.; Vollmer, D.; van Kats, C. M.; van Blaaderen, A. Hollow Silica Spheres: Synthesis and Mechanical Properties. *Langmuir* **2009**, *25*, 2711−2717.
(32) Zhong, Z. Y.; Yin, Y. D.; Gates, B.; Xia, Y. N. Preparation of mesoscale hollow spheres of TiO_2 and SnO_2 by templating against crystalline arrays of polystyrene beads. *Adv. Mater.* **2000**, *12*, 206−209.
(33) Yang, Z. Z.; Gao, S. M.; Li, W.; Vlasko-Vlasov, V.; Welp, U.; Kwok, W. K.; Xu, T. Three-Dimensional Photonic Crystal Fluorinated Tin Oxide (FTO) Electrodes: Synthesis and Optical and Electrical Properties. *ACS Appl. Mater. Interfaces* **2011**, *3*, 1101−1108.
(34) Shundo, A.; Sakurai, T.; Takafuji, M.; Nagaoka, S.; Ihara, H. Molecular-length and chiral discriminations by beta-structural poly(L-alanine) on silica. *J. Chromatogr. A* **2005**, *1073*, 169−174.
(35) Saito, H.; Tabeta, R.; Shoji, A.; Ozaki, T.; Ando, I. Conformational characterization of polypeptides in the solid state as viewed from the conformation-dependent ^{13}C chemical shifts determined by the ^{13}C cross polarization/magic angle spinning method: oligo(L-alanine), poly(L-alanine), copolymers of L- and D-alanines, and copolymers of L-alanine with *N*-methyl- or *N*-benzyl-L-alanine. *Macromolecules* **1983**, *16*, 1050−1057.
(36) Murata, K.; Kuroki, S.; Ando, I. A study of the conformational stability of poly(L-alanine), poly(D-alanine), poly(L-isoleucine), polyglycine and poly(L-valine) and their polypeptide blends in the solid-state by ^{13}C CP/MAS NMR. *Polymer* **2002**, *43*, 6871−6878.
(37) Pinto, M. L.; Mafra, L.; Guil, J. M.; Pires, J.; Rocha, J. Adsorption and Activation of CO_2 by Amine-Modified Nanoporous Materials Studied by Solid-State NMR and $^{13}CO_2$ Adsorption. *Chem. Mater.* **2011**, *23*, 1387−1395.
(38) Xu, X.; Song, C.; Andresen, J. M.; Miller, B. G.; Scaroni, A. W. Novel Polyethylenimine-Modified Mesoporous Molecular Sieve of MCM-41 Type as High-Capacity Adsorbent for CO_2 Capture. *Energy Fuels* **2002**, *16*, 1463−1469.
(39) Qi, G. G.; Fu, L. L.; Choi, B. H.; Giannelis, E. P. Efficient CO_2 Sorbents Based on Silica Foam with Ultra-Large Mesopores. *Energy Environ. Sci.* **2012**, *5*, 7368−7375.
(40) Lowell, S.; Shields, J. E.; Thomas, M. A.; Thommes, M. *Characterization of Porous Solids and Powders: Surface Area, Pore Size and Density*, 4th ed; Springer: Amsterdam, 2006.
(41) Chaikittisilp, W.; Didas, S. A.; Kim, H. J.; Jones, C. W. Vapor-Phase Transport as A Novel Route to Hyperbranched Polyamine-Oxide Hybrid Materials. *Chem. Mater.* **2013**, *25*, 613−622.
(42) Heydari-Gorji, A.; Belmabkhout, Y.; Sayari, A. Polyethylenimine-Impregnated Mesoporous Silica: Effect of Amine Loading and Surface Alkyl Chains on CO_2 Adsorption. *Langmuir* **2011**, *27*, 12411−12416.
(43) Chen, C.; Yang, S. T.; Ahn, W. S.; Ryoo, R. Amine-Impregnated Silica Monolith with a Hierarchical Pore Structure: Enhancement of CO_2 Capture Capacity. *Chem. Commun.* **2009**, 3627−3629.
(44) Bacsik, Z. n.; Ahlsten, N.; Ziadi, A.; Zhao, G.; Garcia-Bennett, A. E.; Martín-Matute, B. n.; Hedin, N. Mechanisms and Kinetics for Sorption of CO_2 on Bicontinuous Mesoporous Silica Modified with *n*-Propylamine. *Langmuir* **2011**, *27*, 11118−11128.
(45) Huang, H. Y.; Yang, R. T.; Chinn, D.; Munson, C. L. Amine-Grafted MCM-48 and Silica Xerogel as Superior Sorbents for Acidic Gas Removal from Natural Gas. *Ind. Eng. Chem. Res.* **2002**, *42*, 2427−2433.
(46) Plaza, M. G.; Pevida, C.; Arenillas, A.; Rubiera, F.; Pis, J. J. CO_2 capture by adsorption with nitrogen enriched carbons. *Fuel* **2007**, *86*, 2204−2212.
(47) Ochiai, B.; Yokota, K.; Fujii, A.; Nagai, D.; Endo, T. Reversible Trap−Release of CO_2 by Polymers Bearing DBU and DBN Moieties. *Macromolecules* **2008**, *41*, 1229−1236.
(48) Rosenholm, J. M.; Duchanoy, A.; Linden, M. Hyperbranching Surface Polymerization As a Tool for Preferential Functionalization of the Outer Surface of Mesoporous Silica. *Chem. Mater.* **2008**, *20*, 1126−1133.
(49) Yu, J. G.; Le, Y.; Cheng, B. Fabrication and CO_2 Adsorption Performance of Bimodal Porous Silica Hollow Spheres with Amine-Modified Surfaces. *RSC Adv.* **2012**, *2*, 6784−6791.
(50) Kassab, H.; Maksoud, M.; Aguado, S.; Pera-Titus, M.; Albela, B.; Bonneviot, L. Polyethylenimine Covalently Grafted on Mesostructured Porous Silica for CO_2 Capture. *RSC Adv.* **2012**, *2*, 2508−2516.
(51) Dillon, E. P.; Crouse, C. A.; Barron, A. R. Synthesis, Characterization, and Carbon Dioxide Adsorption of Covalently Attached Polyethyleneimine-Functionalized Single-Wall Carbon Nanotubes. *ACS Nano* **2008**, *2*, 156−164.
(52) Wang, J. T.; Long, D. H.; Zhou, H. H.; Chen, Q. J.; Liu, X. J.; Ling, L. C. Surfactant-Promoted Solid Amine Sorbents for CO_2 Capture. *Energy Environ. Sci.* **2012**, *5*, 5742−5749.
(53) Bacsik, Z. n.; Atluri, R.; Garcia-Bennett, A. E.; Hedin, N. Temperature-Induced Uptake of CO_2 and Formation of Carbamates in Mesocaged Silica Modified with n-Propylamines. *Langmuir* **2010**, *26*, 10013−10024.
(54) Danon, A.; Stair, P. C.; Weitz, E. FTIR Study of CO_2 Adsorption on Amine-Grafted SBA-15: Elucidation of Adsorbed Species. *J. Phys. Chem. C* **2011**, *115*, 11540−11549.
(55) Hiyoshi, N.; Yogo, K.; Yashima, T. Adsorption characteristics of carbon dioxide on organically functionalized SBA-15. *Microporous Mesoporous Mater.* **2005**, *84*, 357−365.
(56) Knöfel, C.; Martin, C. l.; Hornebecq, V.; Llewellyn, P. L. Study of Carbon Dioxide Adsorption on Mesoporous Aminopropylsilane-Functionalized Silica and Titania Combining Microcalorimetry and in Situ Infrared Spectroscopy. *J. Phys. Chem. C* **2009**, *113*, 21726−21734.
(57) Zheng, F.; Tran, D. N.; Busche, B. J.; Fryxell, G. E.; Addleman, R. S.; Zemanian, T. S.; Aardahl, C. L. Ethylenediamine-Modified SBA-15 as Regenerable CO_2 Sorbent. *Ind. Eng. Chem. Res.* **2005**, *44*, 3099−3105.
(58) Khatri, R. A.; Chuang, S. S. C.; Soong, Y.; Gray, M. Thermal and Chemical Stability of Regenerable Solid Amine Sorbent for CO_2 Capture. *Energy Fuels* **2006**, *20*, 1514−1520.
(59) Pirngruber, G. D.; Leinekugel-le-Cocq, D. Design of a Pressure Swing Adsorption Process for Postcombustion CO_2 Capture. *Ind. Eng. Chem. Res.* **2013**, *52*, 5985−5996.

(60) Berger, A. H.; Bhown, A. S. Comparing Physisorption and Chemisorption Solid Sorbents for Use Separating CO_2 from Flue Gas Using Temperature Swing Adsorption. *Energy Procedia* **2011**, *4*, 562−567.
(61) Pirngruber, G. D.; Guillou, F.; Gomez, A.; Clausse, M. A Theoretical Analysis of the Energy Consumption of Post-Combustion CO_2 Capture Processes by Temperature Swing Adsorption Using Solid Sorbents. *Int. J. Greenhouse Gas Control* **2013**, *14*, 74−83.
(62) Goeppert, A.; Meth, S.; Prakash, G. K. S.; Olah, G. A. *Energy Environ. Sci.* **2010**, *3*, 1949−1960.
(63) Gray, M. L.; Soong, Y.; Champagne, K. J.; Baltrus, J.; Stevens, R. W., Jr; Toochinda, P.; Chuang, S. S. C. CO_2 Capture by Amine-Enriched Fly Ash Carbon Sorbents. *Sep. Purif. Technol.* **2004**, *35*, 31−36.
(64) Li, P.; Ge, B.; Zhang, S.; Chen, S.; Zhang, Q.; Zhao, Y. CO_2 Capture by Polyethylenimine-Modified Fibrous Adsorbent. *Langmuir* **2008**, *24*, 6567−6574.
(65) Patiño-Echeverri, D.; Hoppock, D. C. Reducing the Energy Penalty Costs of Postcombustion CCS Systems with Amine-Storage. *Environ. Sci. Technol.* **2012**, *46*, 1243−1252.
(66) Harlick, P. J. E.; Sayari, A. Applications of Pore-Expanded Mesoporous Silica. 5. Triamine Grafted Material with Exceptional CO_2 Dynamic and Equilibrium Adsorption Performance. *Ind. Eng. Chem. Res.* **2006**, *46*, 446−458.
(67) Gray, M. L.; Hoffman, J. S.; Hreha, D. C.; Fauth, D. J.; Hedges, S. W.; Champagne, K. J.; Pennline, H. W. Parametric Study of Solid Amine Sorbents for the Capture of Carbon Dioxide. *Energy Fuels* **2009**, *23*, 4840−4844.
(68) Jones, C. W. CO_2 Capture from Dilute Gases As a Component of Modern Global Carbon Management. *Annu. Rev. Chem. Biomol. Eng.* **2011**, *2*, 31−52.
(69) Choi, S.; Drese, J. H.; Eisenberger, P. M.; Jones, C. W. Application of Amine-Tethered Solid Sorbents for Direct CO_2 Capture from the Ambient Air. *Environ. Sci. Technol.* **2011**, *45*, 2420−2427.
(70) Choi, S.; Gray, M. L.; Jones, C. W. Amine-Tethered Solid Adsorbents Coupling High Adsorption Capacity and Regenerability for CO_2 Capture From Ambient Air. *Chemsuschem* **2011**, *4*, 628−635.